JTTEE5 10:599-603

Abrasive Wear Resistance of Plasma-Sprayed Glass-Composite Coatings

D.T. Gawne, Z. Qiu, Y. Bao, T. Zhang, and K. Zhang

(Submitted 11 August 2000)

A ball-milled mixture of glass and alumina powders has been plasma sprayed to produce alumina-glass composite coatings. The coatings have the unique advantage of a melted, ceramic secondary phase parallel to the surface in an aligned plateletlike-composite structure. The alumina raises the hardness from 300 HV for pure glass coatings to 900 HV for a 60 wt.% alumina-glass composite coating. The scratch resistance increases by a factor of 3, and the wear resistance increases by a factor of 5. The glass wears by the formation and intersection of cracks, while the alumina wears by fine abrasion and supports most of the sliding load. The wear resistance reaches a maximum at 40 to 50 vol.% alumina, above which there is little further improvement. This critical alumina content corresponds to the changeover from a glass to a ceramic matrix.

Keywords glass coatings, plasma spraying, wear

Introduction

Glasses are extremely versatile materials, easy to process, and capable of producing high-quality surface finishes. Glass also provides effective coatings in many applications owing primarily to its dense structure, corrosion resistance, aesthetic appearance, and low cost.[1] The wear resistance of glass coatings, however, is limited, owing to their relatively low hardness and fracture toughness. This paper is aimed at improving the wear resistance by incorporating alumina into glass coatings during the deposition process. A series of simple mixtures of glass and alumina powders were prepared by ball milling and classification prior to plasma spraying on steel substrates. This paper investigates the deposition, microstructure, and properties of these alumina-glass composite coatings.

Experimental Details

A borosilicate glass (Escol Products Ltd., Huntingdon, United Kingdom) was processed to powder (Corus plc, Port Talbot, United Kingdom) with a particle size range of 38 to 45 μm and oven-dried to remove moisture before spraying. The softening temperature and thermal expansion coefficient of the glass are 430 °C and $14.5 \times 10^{-6}\,K^{-1}$, respectively. The alumina powder was a commercial thermal spraying grade (Metco 105 SF, Sulzer-Metco Ltd., Farnborough, United Kingdom) with a particle size distribution of -25 to 5 μm. The glass and alumina were mixed by ball milling and then classified to give the feedstock powder for plasma-spray deposition. The feedstock powders contained 0, 20, 40, 60, and 100 wt.% alumina with the balance being glass. The substrate material was a low-carbon aluminium-killed sheet steel (Corus plc, Port Talbot, United Kingdom) of 3 mm thickness. The steel substrates were degreased and grit blasted to give a surface with a R_a value of 7 μm immediately before spraying. Spraying was carried out using a Sulzer-Metco plasma spray system with a MBN torch and fluidized bed hopper. The plasma gas and powder-carrier gases were argon-5% hydrogen and pure argon, respectively. An arc power of 29 kW and a spraying distance of 100 mm were used. The feedstock powder was injected into the plasma in front of the nozzle at 90° to the axis of the jet.

The Vickers hardness of the coatings was determined using a Mitutoyu (Mitutoyu (UK) Ltd., Andover, UK) tester with a load of 0.5 N for 15 s. A Teledyne Taber (Taber Industries, North Tonawanda, NY) scratch tester was used to evaluate scratch resistance. This equipment has a conical diamond indenter with an apex angle of 90°. A single unidirectional scratch was made under loads of 0.500 to 5 N, and the width of the scratch was measured using an optical microscope. Wear testing was undertaken in a reciprocating ball-on-flat machine using Alsint alumina balls (Fisher Science Ltd., Loughborough, United Kingdom) of 10 mm diameter. The length of each pass was 12 mm, and the frequency was 60 cycles per minute, giving a distance traveled per cycle of 24 mm. The load applied to the sliding ball was 20 N.

Results and Discussion

Figure 1(a) shows an optical micrograph of a polished cross section of a 20 wt.% alumina-glass coating. The thin, elongated white phase is the alumina splats embedded in a gray glass matrix. The black circles are pores in the glass matrix. The feedstock powders were thoroughly dried before spraying, and the source of the pores or bubbles is attributed to the release of water chemically bound to the glass structure during deposition. The alumina was observed to be uniformly dispersed throughout the glass coating.

A significant observation from Fig. 1 is that the alumina has melted during deposition as well as the glass, despite its considerably higher melting point of 2050 °C, compared with a softening temperature of 430 °C. It is interesting to note how such thermally dissimilar materials can both melt simultaneously in the plasma jet without degradation of one or the incomplete

D.T. Gawne, Z. Qiu, Y. Bao, T. Zhang, and K. Zhang, School of Engineering Systems and Design, South Bank University, London, SE1 0AA, United Kingdom. Contact e-mail: gawnedt@sbu.ac.uk.

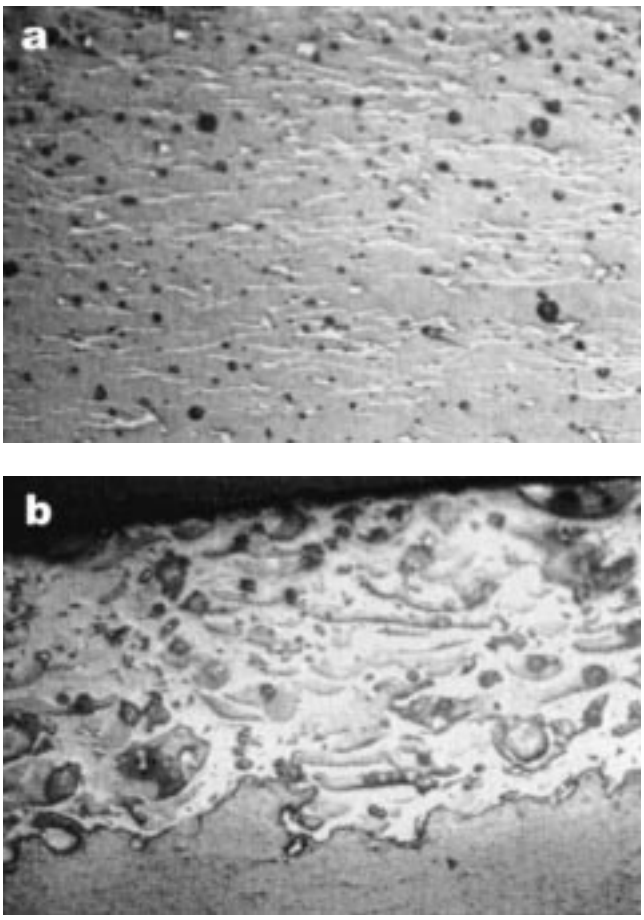

Fig. 1 Polished cross sections of composite glass coatings with (**a**) 20 and (**b**) 60 wt.% alumina

melting of the other. The alumina splats are thin with a large aspect ratio, which indicates a low viscosity and extensive flow of the alumina particles on impact with the substrate.

Figure 1(b) shows a photomicrograph of the 60 wt.% alumina-glass coating, and, here, it is seen that the alumina is the major constituent and the matrix phase. The glass splats are much thicker than those of alumina in Fig. 1(a) and have smaller aspect ratios. This indicates much less flow of glass particles on impact than that of the alumina particles. This is caused by the high silica content of the glass resulting in a strong network-forming tendency and a consequent high viscosity.[1] On the other hand, there is sufficient enthalpy and temperature in the plasma to melt the crystalline alumina particles, and the relatively simple structure of the ionic melt provides a lower viscosity liquid and extensive fluidity at impact.

Figure 2 gives the hardness of the coatings over a range of alumina contents and shows that it conforms approximately to a rule-of-mixture relationship, which is typical of a well-bonded composite material. Microscopic observations on the indentations formed by hardness testing indicate that they were formed by plastic deformation. It is expected that the deformation will take place by shear banding in the softer glass-matrix phase. The shear banding is likely to be initiated by the dilation caused by the stress field at discontinuities, such as surface notches. When the dilation becomes large enough to increase the specific volume to that at the glass transition temperature, the viscosity of the material decreases drastically, and a fluid zone propagates through the sample.[2] The disclike splats of alumina are considered to act as obstacles to shear band propagation and, thus, to raise the stress for plastic deformation. As a result, the hardness is expected to increase with decreasing alumina-splat spacing or increasing alumina content, as found in Fig. 2.

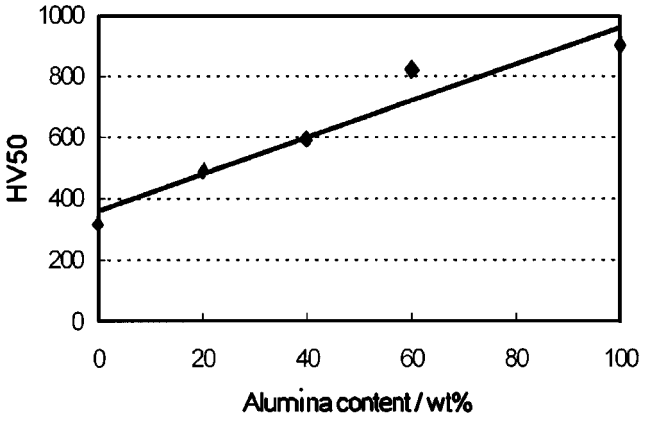

Fig. 2 The effect of alumina content on the hardness of glass-composite coatings

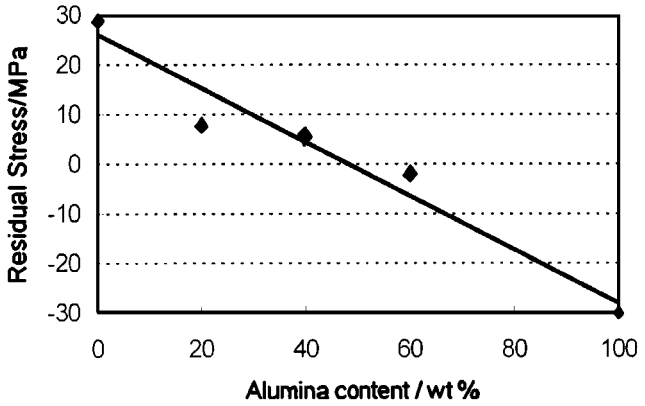

Fig. 3 The effect of alumina content on the residual stress of glass-composite coatings

Figure 3 gives the residual stress of the coatings over the range of alumina contents. The residual stress reduces with increasing alumina and eventually becomes compressive (negative) at 60 wt.% alumina. The residual stress is less than 10 MPa in both the 40 and 60 wt.% alumina coatings. This reduction in residual stress is related to the decrease in mismatch of the thermal expansion coefficient between the coating and the substrate and is discussed by the authors elsewhere.[3]

Figure 4 gives the scratch data for the coatings under an applied load of 5 N. Scratch testing was carried out to complement wear testing because it consists of a single unidirectional pass of the slider over the specimen surface as compared with the much more complex operation of many reciprocating passes in the wear trials. The results show that the presence of alumina produces a major increase in scratch resistance: a content of only 20

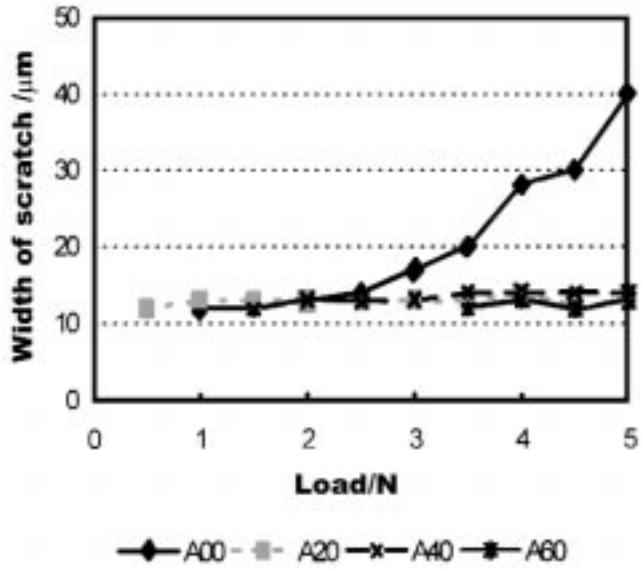

Fig. 4 The groove widths of glass composites after scratch testing under specified loads

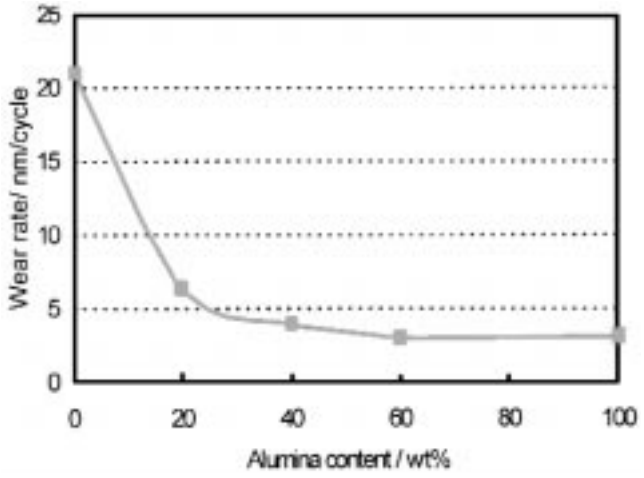

Fig. 5 The effect of alumina content on the wear rate of glass-composite coatings

wt.% alumina reduces the width of the scratch groove to less than a third of that of the pure glass coating.

Sliding wear tests were carried out on the coatings against a loaded alumina ball. An initial period of rapid wear was followed by a more gradual wear stage. The rapid wear is due to the running-in of the two sliding surfaces involving the removal of protrusions, high spots, and misalignments due to the high local stresses. As sliding progresses, the contact stresses reduce, and the wear mode transforms into the milder equilibrium stage. Owing to the inevitable minor variations in setting up the test and in the sample surface finish, the equilibrium wear stage is the more reproducible, and this was used as the indicator of the wear of the coatings.

Figure 5 shows the influence of alumina content on the sliding wear rate of the glass composite coatings. The wear resistance reduces substantially for alumina additions up to

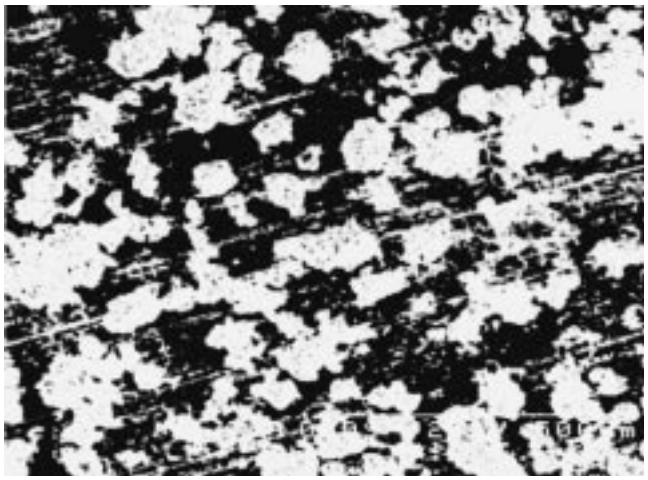

Fig. 6 Scanning electron microscopy (SEM) micrograph of the worn surface of a 40 wt.% alumina-glass composite coating

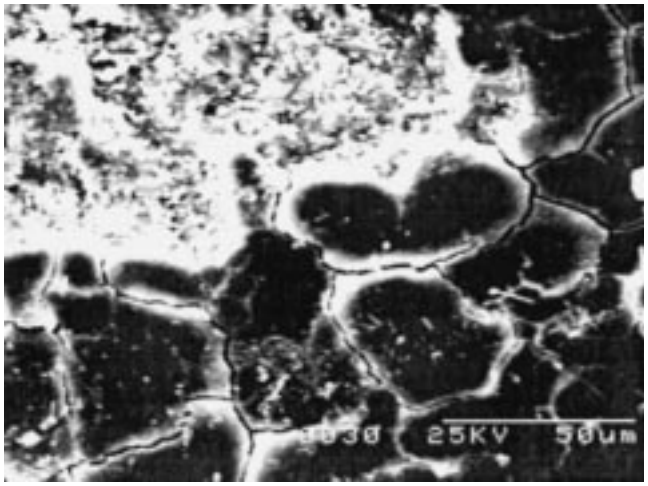

Fig. 7 An SEM micrograph showing the crack network in the glass (dark phase) matrix on the worn surface of a 40 wt.% alumina-glass coating

approximately 50 wt.%, and, thereafter, there is little further improvement. Figure 6 gives the worn surface of a 40 wt.% alumina-glass coating and shows alumina (the white phase) splats in a darker glass matrix. Closer examination of the coating reveals that the glass phase contains a pronounced crack network, as shown in Fig. 7. The pure glass coatings also exhibit crack networks on their worn surfaces. This contrasts with the behavior in hardness testing, which did not generate visible cracks around the indentations in the glass phase. However, the sliding action modifies the stress field and, in particular, introduces a significant tensile component immediately behind the moving slider.[2–4] This combines with the biaxial-tensile residual stress already present (as a result of thermal stresses generated during deposition[1]) to initiate cracks normal to the sliding surface and to create the observed network.

Further microstructural observations, particularly after prolonged sliding, show that the individual cells of the crack net-

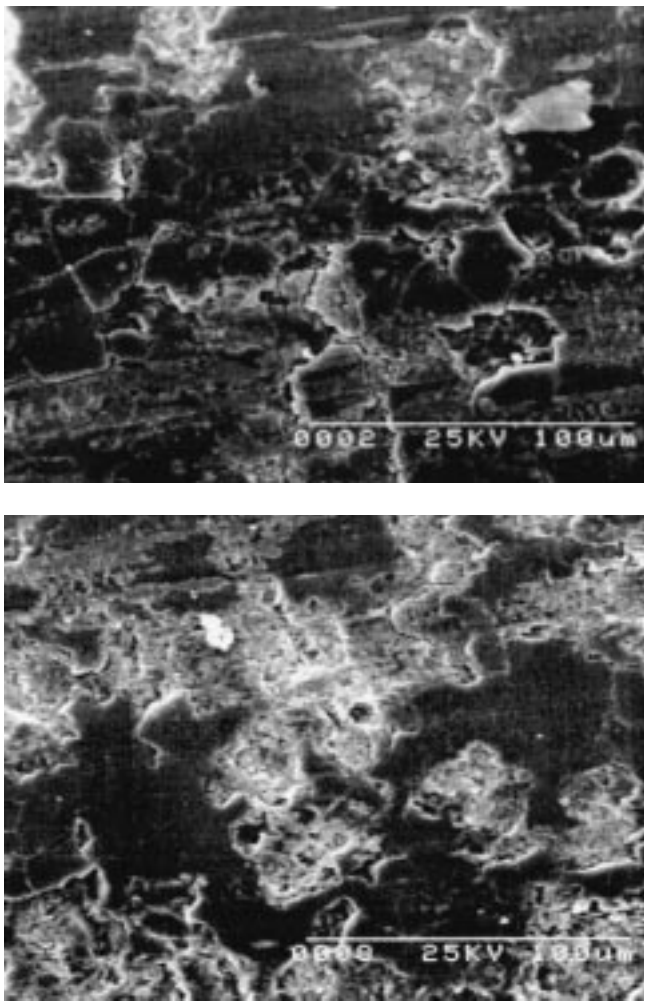

Fig. 8 An SEM micrographs of the worn surface of a 40 wt.% alumina-glass coating showing the formation of platelet debris

work tend to fragment as thin platelets and form wear debris, as shown in Fig. 8. This detachment process requires cracks to propagate parallel to the sliding surface in order to link with the normal cracks and form platelets. Idealized stress analysis on static indentation and its extension to sliding contacts[5–7] indicates that lateral cracks can initiate from the bottom of the plastic zone in the coating beneath the slider and then propagate parallel to the free surface before turning upward to form a detached platelet. A further possibility is that the material at the edges of the cracks in the network becomes slightly raised due to the stress perturbations in the sliding system. These edges are then struck by a returning reciprocating slider resulting in a lifting action or a shearing action, which initiates cracks parallel to the sliding surface.

Examination of the alumina on the worn surfaces of the composite coatings shows little evidence of visible, large-scale cracking, and cracks in the glass matrix do not propagate into the alumina, as shown in Fig. 7. This is expected to be a consequence of the higher strength and fracture toughness of alumina as compared with glass. This is reflected in the higher hardness (Fig. 2) and wear resistance (Fig. 4 and 5) of alumina. Material removal from the alumina splats appears to have occurred mostly by fine abrasive wear: plastic deformation followed by microfracture.

The wear of the alumina-glass composite coating is considered to take place in two stages. The glass wears rapidly to leave the alumina slightly raised above the mean surface level. The alumina then becomes the sole contacting surface and wears at a much lower rate than the glass. The alumina splats are adequately supported by the glass matrix because much of the stress field imposed on the surrounding matrix is compressive, which acts to suppress cracking. The larger the volume or area fraction of the alumina phase at the coating surface, the less the true contact stresses and the lower the wear rate. In reality, the wear of alumina and glass averaged over the entire specimen surface is likely to occur simultaneously rather than sequentially. The resultant wear resistance will be dominated by the stronger alumina as this phase will support the applied sliding load for the majority of the wear process.

Figure 5 indicates that above approximately 50 wt.% alumina in the coatings there is little further improvement in wear resistance. Figure 1(b) is a micrograph of a cross section of a 60 wt.% alumina-glass coating and indicates that the matrix phase is now alumina rather than glass. The coating consists of glass splats in a surrounding alumina phase. The glass splats are much thicker and have a smaller aspect ratio than the alumina splats in Fig. 1(a), which is a result of their higher melt viscosity, as discussed previously. It is also noted that, because of the higher density of alumina, 60 wt.% alumina corresponds to only 49% alumina by volume, the matrix changeover takes place below 50 wt.%. This is again expected to be a result of the low melt viscosity of alumina relative to the glass, which enables it to flow around a second phase and readily form a matrix.

Figure 5 shows that the coatings with more than 50 wt.% alumina have similar wear resistance to that of the pure alumina coatings. Cracks initiating in isolated glass splats are prevented from propagating to other glass splats by the surrounding alumina matrix. However, it is still surprising that the weaker glass phase does not adversely affect the wear resistance of the composite. The glass splats contain pores, and these are known to benefit strain tolerance in zirconia coatings.[8] It is thus possible, therefore, that the porosity in the glass splats improves the strain tolerance of the composite coating and compensates for their lower strength.

Conclusions

1. Alumina-glass composite coatings containing up to 60 wt.% alumina have been successfully plasma sprayed from feedstock consisting of simple ball-milled mixtures of glass-alumina powders.

2. The alumina melted in the plasma as well as the glass and flows extensively to form splats in an aligned platelet-composite structure.

3. The alumina increases the hardness from 300 HV for a pure glass coating to 900 HV for a 60 wt.% alumina-glass coating.

4. The alumina increases the scratch resistance by a factor of 3 and the sliding wear resistance by a factor of 5.

5. The wear resistance reaches a plateau at 40 to 50 vol.% alumina, which corresponds to the changeover from a glass matrix to an alumina matrix.

6. The wear resistance of the alumina-matrix composite coatings is similar to that of pure alumina coatings.

Acknowledgments

The research was sponsored by the Engineering and Physical Sciences Research Council and the Department of Trade and Industry under the LINK Programme for Surface Engineering. The work was carried out in collaboration with Corus plc and Escol Products Ltd. The authors thank the preceding for their support and permission to publish this paper.

References

1. H. Rawson: *Properties and Applications of Glass*, vol. 3, *Glass Science and Technology*, Elsevier, Amsterdam, 1980.
2. D.T. Gawne and U. Ma: *Mater. Sci. Technol.*, 1987, vol. 3, pp. 228-338.
3. T. Zhang, Z. Qui, Y. Bao, D.T. Gawne, and K. Zhang: in *Thermal Spray: Surface Engineering via Applications*, Christopher C. Berndt, ed., ASM International, Materials Park, OH, 2000, pp. 355-40.
4. N.P. Suh: *Wear*, 1977, vol. 44, pp. 1-7.
5. F.T. Barwell: *Wear*, 1985, vol. 90 (1), pp. 164-72.
6. N.P. Suh: *Tribophysics*, Prentice-Hall, Englewood Cliffs, NJ, 1986.
7. B.R. Lawn and M.V. Swain: *J. Mater. Sci.*, 1975, vol. 10, pp. 655-656.
8. H. Herman: *Scientific American*, 1988, vol. 259, pp. 112-19.